Computational Fluid Dynamics Modeling and the Transport of Cough Particles in an Aircraft Cabin

Angela C. Davis, Malia Zee, Andrew D. Clark, Tateh Wu, Daniel J. Menard, Stephen P. Jones, Lindsay L. Waite, Robert J. Atmur, Joshua J. Cummins, Nels A. Olson

Abstract

The medical community continues to study the required dose and time of exposure necessary to cause an infection with SARS-CoV-2 and in some cases other respiratory diseases as well. The industry thus needs a way to quantify exposure in an aircraft cabin that can be easily understood and will not change as the medical science is further settled. The mass of expiratory particles emitted by an index infectious passenger's cough that are then inhaled by nearby susceptible passengers was selected as that quantifiable parameter. To establish the mass inhaled, computational fluid dynamics (CFD) analysis was used. Initial conditions in the aircraft cabin, along with air flow velocity, direction of air flow, volumetric air exchange rate, particle mass upon emission, evaporation, surface deposition, and particle dynamics were accounted for by the CFD models. Inputs to the modeled environment have been presented. These parameters were taken from the literature and adjustments were made based on the current understanding of droplet dynamics in the atmosphere e.g., once a particle interacts with a surface it is removed from the airborne portion of the model. The values predicted by the CFD models were compared against those from a test recently published by the Transport and Air Mobility Command of the United States Military.

Introduction

The primary purpose of this paper is the analysis of respiratory particles that carry pathogens emitted by a coughing infectious index passenger. The focus is on particle transport and removal in the aircraft cabin. Larger size particles may be removed by the force of gravity or by striking surfaces via their inertia, while smaller particles (aerosols) may remain airborne until they are removed by the environmental control system (ECS). The cabin, including the ECS, is designed for thermal comfort of passengers and also functions as an engineering control for particle exposure of passengers. This study focuses on a perturbation model where a cough is emitted by a passenger. The cough was selected because the number and volume of particles emitted by coughing is larger than that associated with emission by breathing or talking. Sneezing was not selected because symptoms of SARS-CoV-2 in general do not include an increased incidence of sneezing.[1] Estimates are made for mass inhaled by susceptible passengers via a set of CFD models and empirically derived data; thus providing a measure that will remain constant while the biological reality of infection dynamics is settled.

Aircraft Cabin Design

The Boeing airplane cabin ventilation design meets the FAA requirement for ventilation (14 CFR § 25.831)[2], in addition to in-house proprietary air flow requirements. The passenger cabin air supply typically consists of 50% outside air and 50% filtered recirculated air to provide humidity with the air being mixed before being distributed to the passenger cabin. The air is supplied into the passenger cabin through air distribution nozzles, which are typically located above the seats to maximize thermal comfort for passengers and crew (Figure 1). On the 737 Boeing Sky Interior (BSI), air distribution nozzles are located outboard of the Passenger Service Unit (PSU) and direct the air flow inboard towards the

center of the passenger cabin as shown in Figure 2. The stream of supply air stays attached to the PSU and stow-bin by virtue of the Coandă effect.[3]

The combined stream is forced towards the floor, leading to a region of relatively high velocities in the aisle area compared to the region around the passengers' seats. This downwards motion can be aided by buoyancy, if the supply air flow is at a colder temperature than the bulk cabin air temperature. Upon reaching the floor level, the stream splits to move outboard towards the return air grilles on either side (Figure 1). A lower pressure differential behind the return air grille helps pull air flow through the grille. The recirculated air is passed through high-efficiency particulate air (HEPA) filters to remove particles, including those carrying viruses, at an efficiency of 99.97% at the most penetrable particle size of 0.3 μm (Figure 2). This is sufficient to remove pathogens including viruses that are contained in the dried out droplet nuclei of respiratory emissions.[4,5]

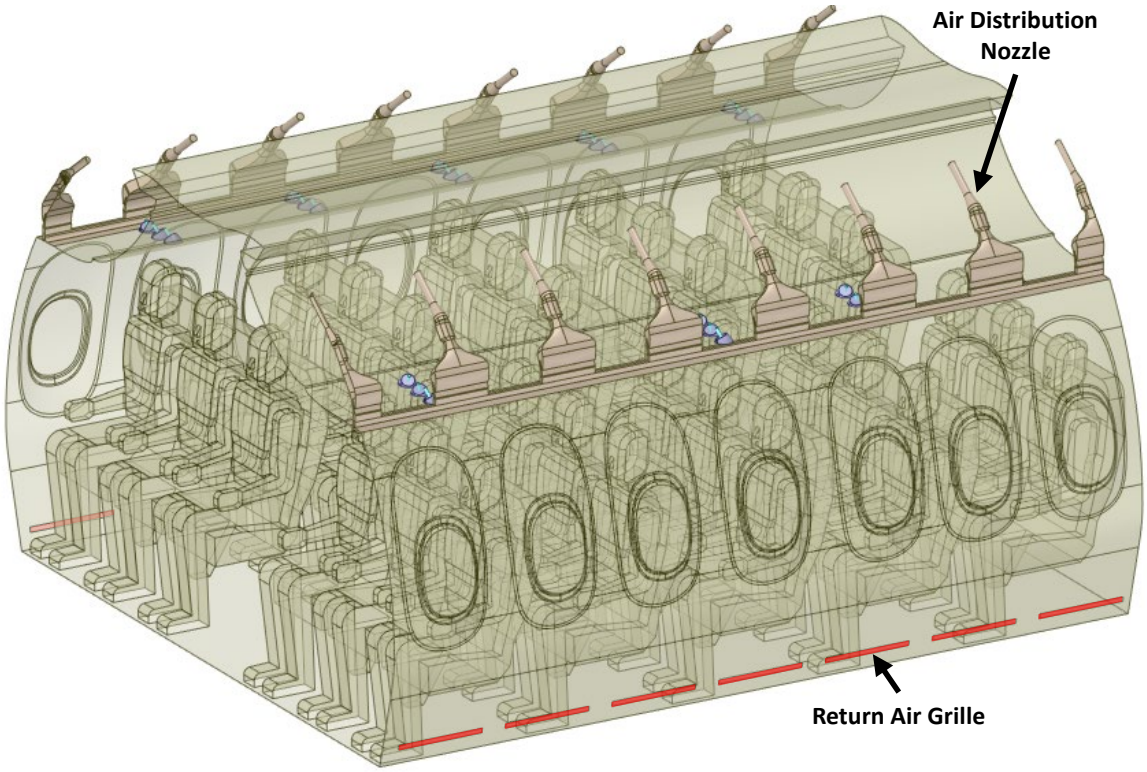

Figure 1. 737 BSI five-row cabin model used in simulations, with ventilation features highlighted.

The remaining air that has not left the passenger cabin becomes entrained in the high velocity jet at the air distribution nozzle, aided in direction by the buoyancy forces created by heat sources (e.g., passengers and In-Flight Entertainment Systems, depicted by the dotted arrows in Figure 2).

The resulting air flow patterns illustrate two defined counter-rotating air flow cells on either side of the passenger cabin (Figure 2). The center of the counter-rotating cells has been shown to shift on a time-dependent basis while the overall flow pattern structure remains stable. The effects of these random shifts are also assessed in this study.

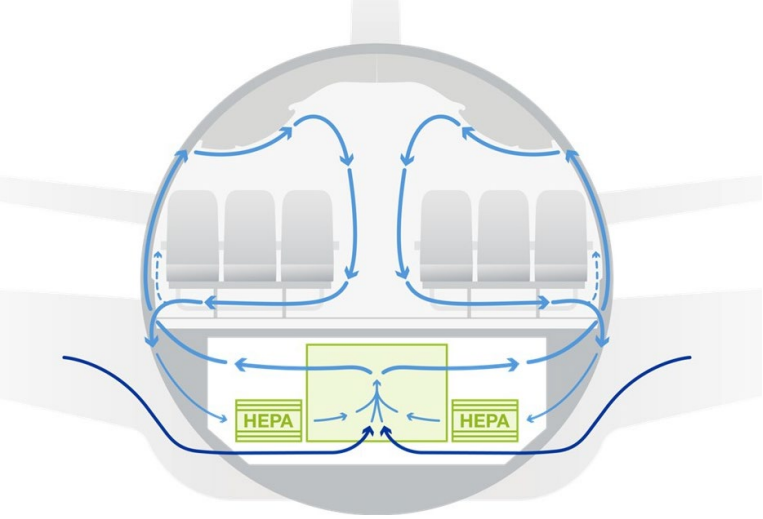

Figure 2. Idealized air flow in the passenger cabin

Directional air flow from top to bottom with minimal fore/aft flow limits the particle spread in the cabin. The positioning of passengers further reduces air flow between rows fore and aft, and the high back seats also act as barriers similar to those now commonly seen in other environments.

Methods

Model Configuration

To quantify the mass inhaled by nearby passengers, a five row section of a 737 BSI cabin was selected as the built environment, as shown in Figure 1. This model was implemented on a typical single aisle aircraft with three seats on either side of the aisle. The 737 BSI cabin model includes thirty seats occupied with numerical manikins. A one cubic foot breathing zone measurement volume shown in Figure 3 was defined around the head of each numerical manikin to track exposure. Note that the CFD model was generated with all seats filled resulting in a load factor of 1.0. Changes in the air flow pattern due to a seat being left empty are not addressed in this study. In the simulations presented herein, masks are not considered.

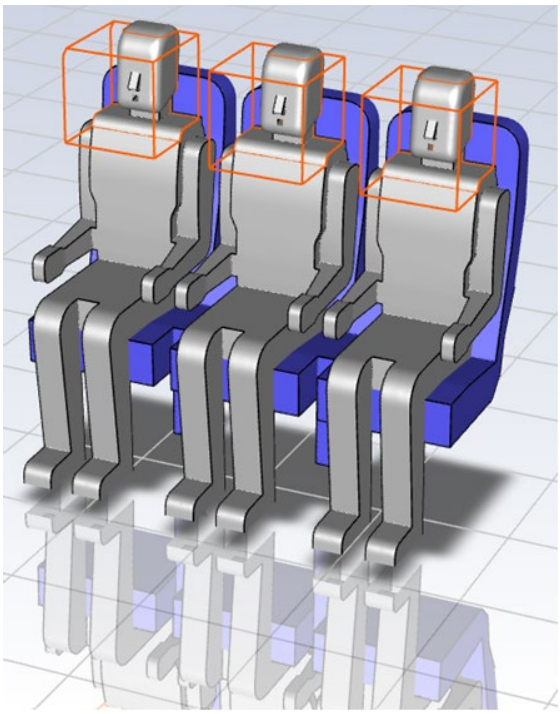

Figure 3 Breathing zone measurement volume defined around the head of each numerical manikin

The nozzle supply can be bypassed by the adjustable Personal Air Outlets (PAOs) that are located in the overhead Passenger Service Unit (PSU). For this study, the PAOs were left in the off-position due to the lack of a definitive recommendation for PAO utilization.

CFD Simulation

A CFD analysis was conducted using ANSYS Fluent™ 19.2 and consisted of a passenger emitting particles (a coughing index passenger who does not cover their mouth or wear a mask when they cough). Expiratory cough particles were released by numerical manikins either in seat 3D (aisle seat), 3E (middle seat) or 3F (window seat) in each CFD simulation. The cough consisted of 106 million particles released in 0.4 seconds by an assumed index passenger.[6,7] This large number of particles would have required weeks of computational time to track accurately, even with thousands of core processors allocated. For that reason, the number of particles was reduced by a factor of 157 to 676,000. These particles were then represented by 34,550 parcels, and tracked in the cabin via Fluent Discrete Phase Model (DPM) for the transient CFD cough simulation. Upon completion of the simulation, the mass of particles that entered the breathing zone of each passenger, and those deposited on surfaces, were multiplied by 157 to bring the total mass back to that originally required i.e., 106 million expiratory particles.

The required air flow and thermal boundary conditions for CFD simulation are listed in Table 1. Both at cruise inflight conditions and on the ground conditions are covered by these ranges. The steady-state solutions of the cabin CFD were used as the initial conditions for the subsequent transient simulation. The unsteady Reynolds-averaged Navier-Stokes (URANS) approach was used to predict transport of poly-dispersed droplets emitted from an index passenger. The supply air temperature was varied to maintain a targeted 75°F cabin temperature at different flow rates (Table 1).

Particles were tracked over 13.3 M mesh positions, with each time step lasting 0.05 seconds after the initial expiratory cough event thereby using shorter time steps to accurately model the higher flow rate of the cough.

Table 1 Air flow and thermal boundary conditions for the 737 BSI cabin CFD simulation

	Condition
Supply flow rate [Actual ft^3/min]	323 – 588
Return flow rate [Actual ft^3/min]	Same as supply
Relative humidity	0% - 20%
Occupant heat generation [W]	2100 (70W/occupant)
Sidewall [°F]	55 – 65
Stowage bins, Ceiling, Floor	Adiabatic walls
Front and Back interfaces	Periodic
Nozzle supply air temperature [°F]	62 – 67
Cabin average temperature [°F]	75 – 77

The Realizable k-ε turbulence model with Fluent Enhanced Wall Treatment was used for the turbulence modeling. The expiratory particle transport was simulated using Fluent Discrete Phase Model (Lagrangian scheme). In this simulation, thermal radiation heat transfer and the evaporation of the expiratory particles were included to realistically address the cabin environment. The mixture of air and water vapor (i.e., the continuous phase) was solved using the Eulerian scheme. Here, interactions between the droplets and air flow such as momentum and heat transfer were included.

Evaporation of the water component of the droplets is calculated and is part of the overall CFD analysis. The modeling software calculates the evaporation by a combination of expiratory temperature (87.8°F, 31°C), vapor pressure, cabin air temperature, and velocity. The vapor pressure of the aerosols and droplets was adjusted for the effect of lung surfactants. Vejerano (2018)[8] demonstrated that the effect was a continuous factor on the speed of evaporation while a correction multiplier of 0.28 was used to correct the vapor pressure of the expiratory particles. The particles were also assumed to have a volatile fraction of 90%. Therefore, none of the droplets evaporated completely and the droplet size was reduced over time until reaching the 10% non-volatile fraction.

The Cough

To simulate a human cough in a cabin environment, the methodology developed by Gupta (2009)[9] was adopted and combined with updated droplets size distribution and number concentrations from Zayas, (2012).[6] These data along with the Cough Peak Flow Rate (CPFR), Peak Velocity Time (PVT), and Cough Expired Volume (CEV) are detailed in the Supplemental Information and Supporting Data for this paper. There is expected to be significant individual variation so the choice of these parameters was based on the best available information from the literature. Of the many estimates available in the literature, the Zayas (2012)[6] data was selected due to its inclusion of the smaller particles (down to 0.1 µm) and the much higher number density of particles identified by the use of the Malvern Spraytec™ instrument.

Approximately 0.0544 µL (or 54.4 µg) before-evaporation-of-effluent was generated by the index passenger during a single cough. The cough particle removal from the cabin and the mass of expiratory particles inhaled by susceptible nearby passengers were calculated.

The expiratory particle mass deposited/accreted on surfaces in the cabin (e.g., interior panels, seats, manikins, floor, etc.) was modeled and monitored with the assumption that the particle mass remains

trapped on the surface upon impact. The loss of expiratory particles to surfaces is inherent in the decay of mass loss over time for the entire cabin.

Inhalation

To determine the mass of particles inhaled, first the total nonvolatile (droplet nuclei) mass in the breathing zone was determined at each time point per Equation 1.

$$m(t) = \sum_{i=1}^{38} N_i(t) * m_i \qquad \textit{Equation 1}$$

In this Equation, $m(t)$ is the time dependent nonvolatile mass in the breathing zone, $N_i(t)$ is the number of particles at droplet size i in the breathing zone at time t, and m_i is the nonvolatile mass of droplet size i. Next, the nonvolatile mass was converted to volume assuming the density of pure water.

To incorporate time dependent breathing as applied to each passenger, Equation 2 was utilized to calculate the inhalation portion of a sinusoidal tidal breathing curve[10] as depicted in Figure 4. Figure 4 shows the tidal breathing inhalation volumetric flow rate in liters per second.

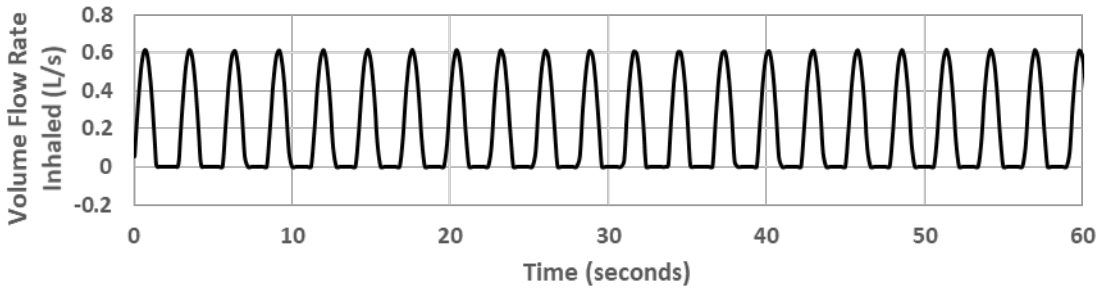

Figure 4. Inhalation portion of tidal breathing volumetric flow rate versus time

$$IR(t) = \begin{cases} A\ sin(B(t+C)), 0 < B(t+C) < \pi \\ 0, \pi \leq B(t+C) \leq 2\pi \end{cases} \qquad \textit{Equation 2}$$

The following height and weight inputs and the equation provided by Gupta (2010)[10] were used to calculate the magnitude of the amplitude, A, and period, B. The phase shift, C, was varied to obtain the maximum nonvolatile volume inhaled. For an average US male with a weight of 89.7 kg and height of 1.75 m [11] A is equal to 0.616 L/s, and B is equal to 2.23 s^{-1}. Significant variation in the volume of inhalation is expected between individuals, and the time at which inhale occurs will affect the total volume of particles inhaled.

The breathing zone was assumed to be well mixed, a simplifying assumption not expected to bias results. Utilizing Equation 3, the fraction of the breathing zone volume inhaled was multiplied by the total volume of particles in the breathing zone to provide a time dependent particle volume inhalation rate for each passenger Figure 5(a), and integrated over time to obtain the total volume inhaled Figure 5(b).

$$V_{inhaled} = \int_0^{t_f} V(t) * \frac{IR(t)}{V_{bz}}\, dt \qquad \textit{Equation 3}$$

In Equation 3 $V_{inhaled}$ is the total volume of nonvolatile cough particles inhaled, $V(\mathrm{t})$ is the volume of nonvolatile particles within the breathing zone at time (t), and V_{bz} is the volume of air in the breathing zone, 22.7 L.

The total nonvolatile volume and mass inhaled were calculated for all passengers excluding the cougher.

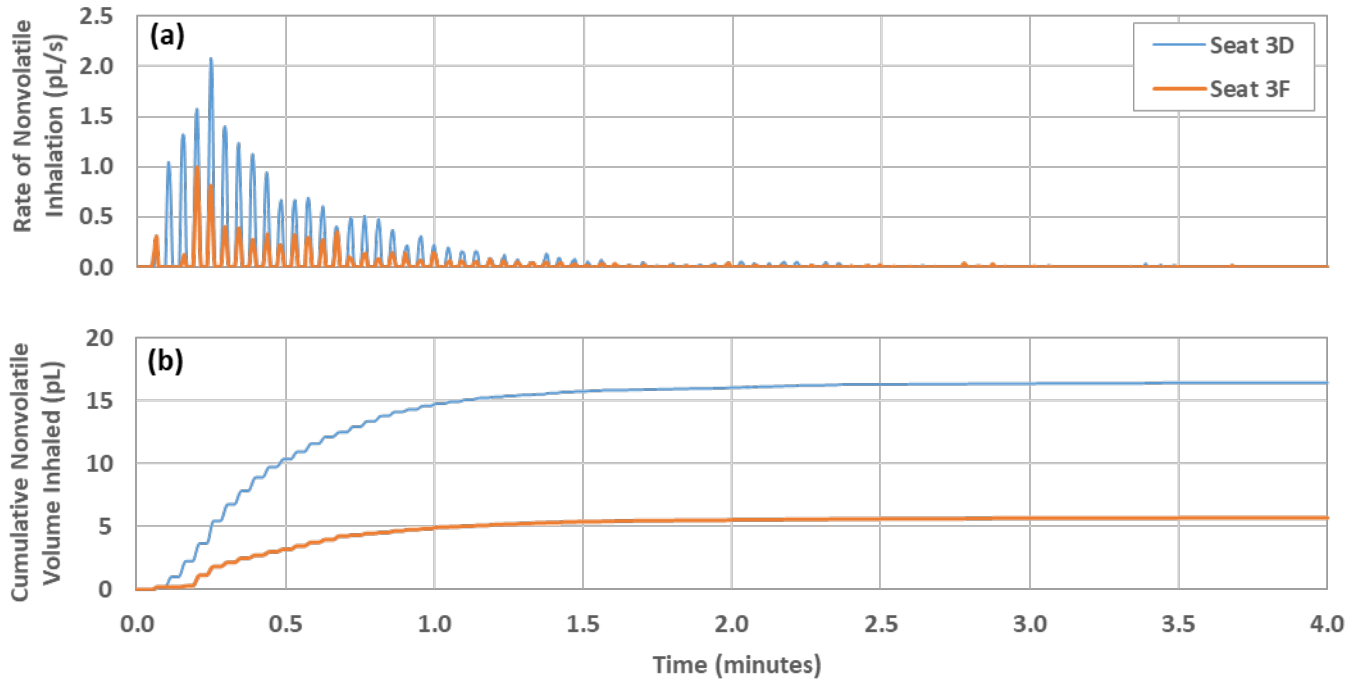

Figure 5. The nonvolatile volume inhalation rate was integrated with respect to time, providing the total nonvolatile volume of inhaled cough particles, Equation 3. (a) Nonvolatile volume inhalation rate and (b) cumulative nonvolatile volume inhaled versus time for susceptible passengers in seats 3D and 3E with an index passenger in seat 3E.

Air flow Conditions and CFD Setup

Seven simulations were run, varying the initial air flow condition, the air supply flow rate, and the location of the coughing index passenger, as shown in Table 2.

Table 2 Case Summary of the 737 BSI 5-row cabin CFD simulation, cubic feet per minute (cfm)

Flow Rate	Flow Rate (cfm)	Initial Condition	Index Passenger Seat
100%	588 cfm	Initial Condition 1, 0 sec. offset	3D
100%	588 cfm	Initial Condition 2, 90 sec. offset	3D
100%	588 cfm	Initial Condition 3, 120 sec. offset	3D
77%	453 cfm	Initial Condition 4, 0 sec. offset	3D
55%	323 cfm	Initial Condition 5, 0 sec. offset	3D
100%	588 cfm	Initial Condition 1, 0 sec. offset	3E
100%	588 cfm	Initial Condition 1, 0 sec. offset	3F

The complex steady-state air flow of an aircraft cabin for cruise conditions was used as the initial air flow condition prior to the release of expiratory cough particles. Figure 6 shows the three initial condition air flow patterns evaluated for the 100% flow rate condition, where the highest speeds are shown in red and the lowest in blue. Each of the three supply air flow rates studied required a different initial steady state solution, and one air flow condition was studied with initial conditions from three different time instances.

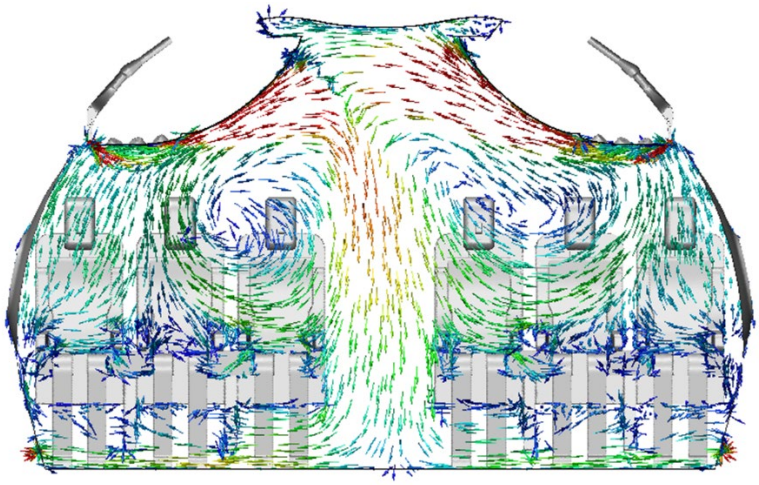

(a) Initial Condition

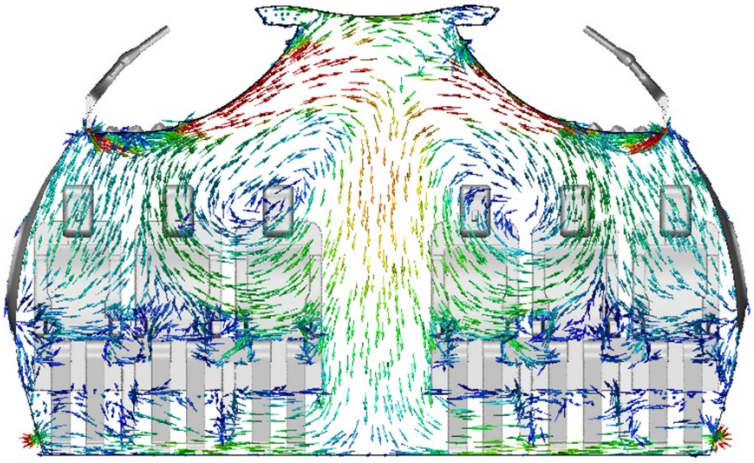

(b) Initial Condition at Time = 90 Seconds

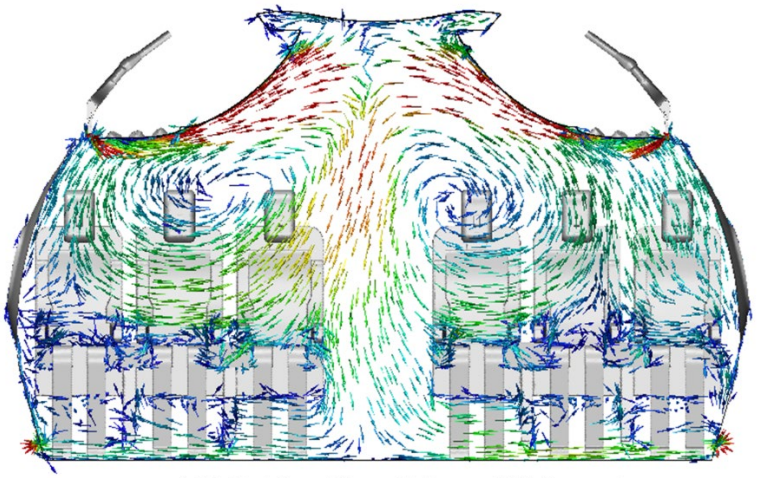

(c) Initial Condition at Time = 120 Seconds

Figure 6. CFD air flow initial air flow conditions snapshots highest speed shown in red, lowest in blue. (a) Taken at time zero, (b) taken at time 90 seconds, (c) taken at 120 seconds

Results

Particle Removal Dynamics

Overall particle dynamics were tracked by following the decay in the number of expiratory particles over the course of each simulation, Figure 7. The initial features on the decay curves correspond to deposition onto surfaces such as the seat back in front of the index subject. Overall, approximately 50% of the nonvolatile content was deposited on various surfaces, with the rest removed by the ECS.

Differences due to random fluctuations of the flow field were captured effectively by differences in starting conditions and affected the rate of particle removal from the cabin over the first 1-2 minutes, Figure 7(a). However, these differences decreased with time, and the final time for particle removal was independent of the initial condition. For an index passenger in seat 3D with ventilation at 100%, initial conditions resulted in a 3-second difference in the time to reach 95% removal of particles in the cabin, which was 2.4 minutes.

Supply air flow rate, on the other hand, had a large effect on the rate of particle removal, Figure 7(b). At 100% flow rate, 95% of the particles were removed in 2.3-2.5 minutes (80% in 1.3-1.4 min, 99% in 3.3-3.5 min). At 55% flow rate, it took 4.5 minutes to reach 95% removal of particles (80% in 2.6 min, 99% in 6.3 minutes).

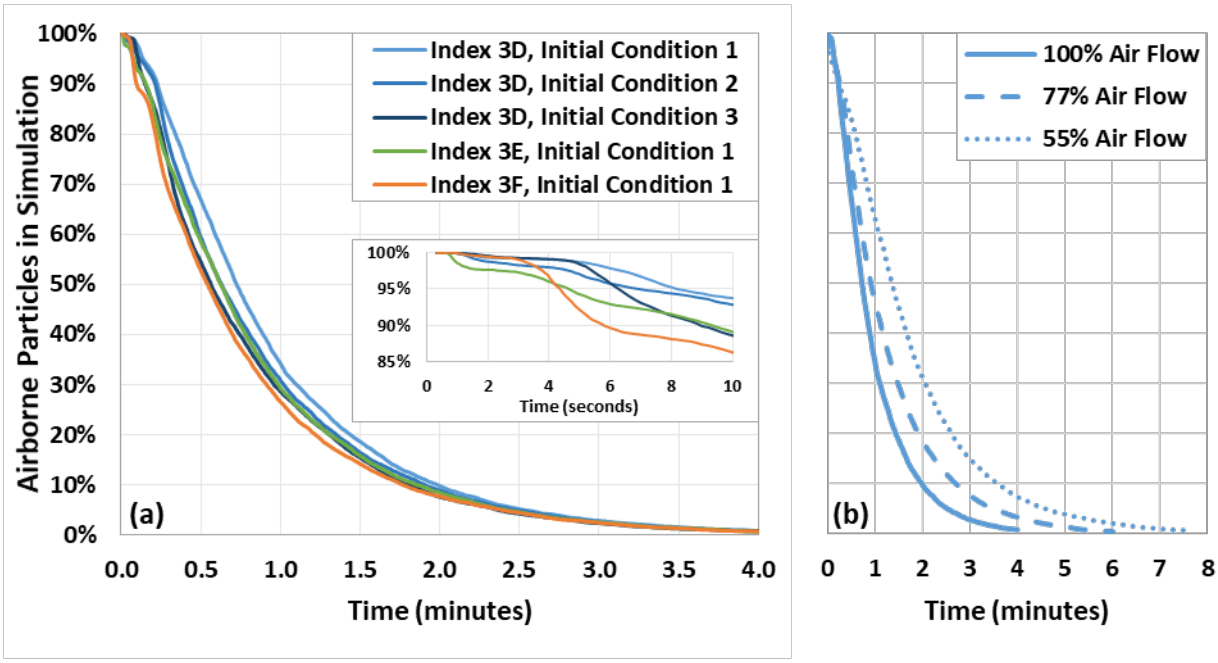

Figure 7. Decay of expiratory particles over time after initial release. (a) Ventilation at 100% of flow rate with different index seats and initial conditions. (b) Ventilation at 55-100% of flow rate with index subject in seat 3D.

Particle dynamics in the breathing zones of susceptible passengers were tracked by following their mass over time. Masses were used instead of particle counts, and since all particles were dehydrated by the time they reached the nearby breathing zones, masses are expressed as a percentage of the original nonvolatile content, Figure 8.

Note: The mass inhaled is reported as the droplet nuclei mass, to obtain the expiratory mass one must multiply by 10.

Particle decay in a given breathing zone was faster than the overall rate of particle removal. For an index passenger in seat 3E, susceptible passenger in seat 3D, and 100% air flow, 95% of the cumulative nonvolatile mass was removed in 1.4 minutes (80% in 0.7 min, 99% in 2.3 min). A seat chart is provided in Figure 9.

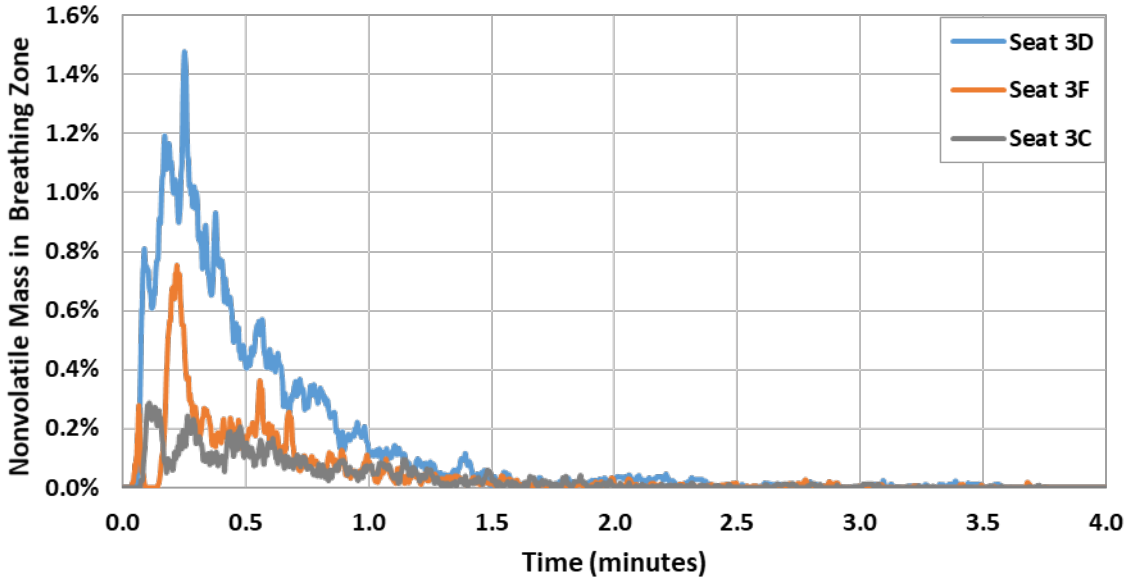

Figure 8. Mass of expiratory material released by index subject in seat 3E and present in the breathing zones of susceptible subjects in nearby seats over time after initial release.

1A	1B	1C	1D	1E	1F
2A	2B	2C	2D	2E	2F
3A	3B	3C	3D	3E	3F
4A	4B	4C	4D	4E	4F
5A	5B	5C	5D	5E	5F

Figure 9. Seat chart for the 5-row section used in the model, highlighting seats occupied by the index subject in different simulations.

Inhaled Mass

Inhaled mass in each susceptible passenger's breathing zone was integrated over the course of each simulation, Figure 10. In general, passengers seated closer to the index seat had a higher exposure to index expiratory material than those farther away. Exposure was highest for passengers seated in the index row, and lowest for passengers seated two rows away. Exposure was higher on the right side of the cabin, where the index seat was located, than the opposite side.

Exposure of susceptible passengers in the index row was lowest when the index subject was in the window seat. Exposure of passengers in the window seat was lower than exposure of passengers in the aisle seat. However, all exposures were a small fraction of the amount released: the maximum mass inhaled by a susceptible passenger was 0.3% (Supplemental Figure 13 and Figure 14). This occurred for

index passenger in seat 3E and susceptible passenger in seat 3D, with dynamics shown in Figure 8. Differences due to random fluctuations of the flow field had a substantial effect on exposure for some of the seats, with the maximum coefficient of variance of 45%, which occurred for susceptible passenger in seat 3F. The minimum coefficient of variance was 5.4% and the average was 19%.

Reducing the ventilation flow rate from 100% of flow to 55% resulted in a wider spread of particles throughout the cabin, observed as an increase of inhaled mass for all rows in Figure 10(c) compared to Figure 10(a). For most passengers, exposure increased as ventilation was reduced. As one exception, when ventilation was reduced to 77%, exposure of seats 3A-C slightly decreased. However, this exception is thought to be due to random differences in initial conditions used for each ventilation flow rate.

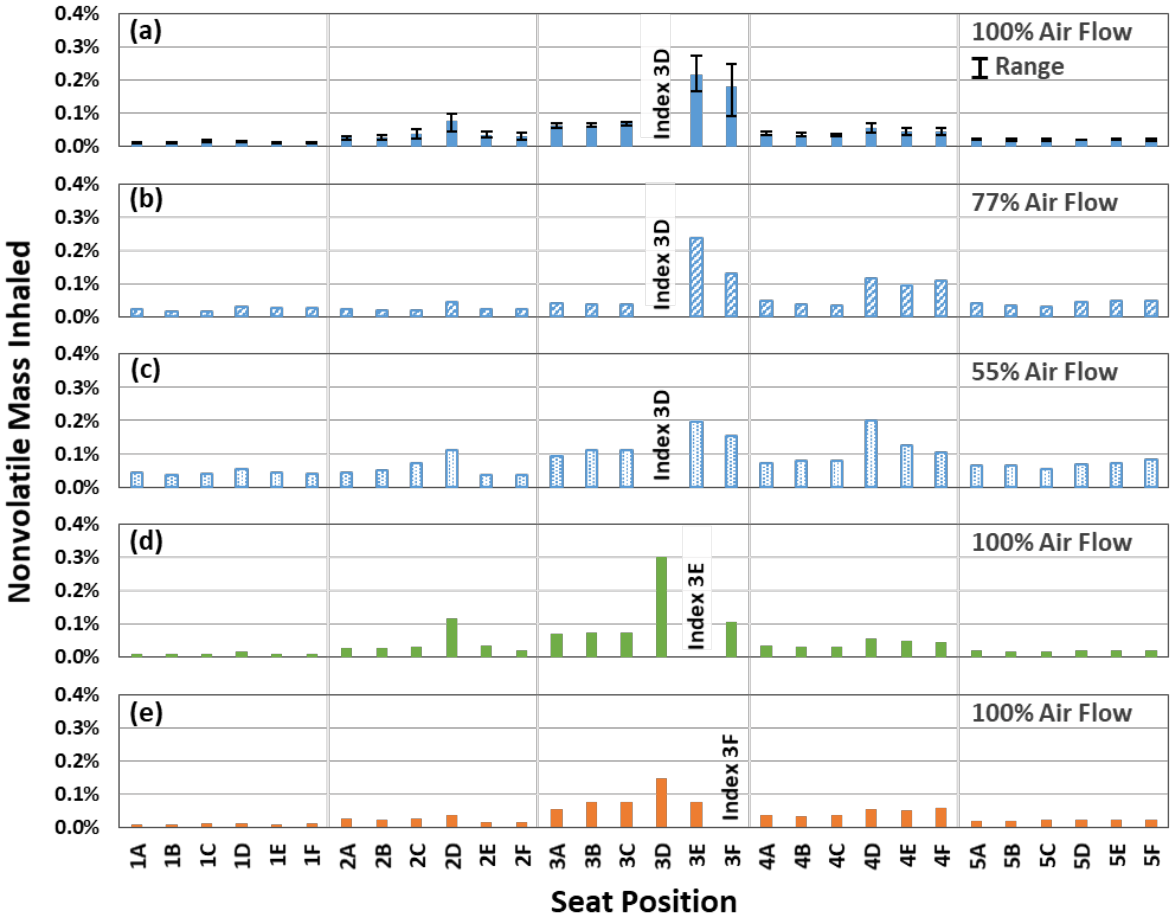

Figure 10. Mass of expiratory material inhaled by susceptible subjects in different seats for different ventilation conditions (a-c) and different index seat positions at 100% air flow (a, d-e). Error bars in (a) represent the range over three different initial conditions.

Discussion

Transport of particles expelled by a single cough was studied to characterize the effectiveness of an airplane ventilation system in protecting passengers from exposure to an infected index case. This case was studied as a perturbation to quantify the efficacy of the aircraft ventilation system in removing the released particles from the cabin, and as a scenario that currently commands public interest. While highly symptomatic COVID-19 carriers are unlikely to be on commercial aircraft due to current airline

travel policies, lightly symptomatic carriers are able to board undetected and do so with some regularity. According to contact tracing organizations,[12] this occurs when the subject becomes infectious while away on travel, and travels while potentially symptomatic in order to return home. Nonetheless, reports of COVID-19 transmission onboard aircraft are rare, with no confirmed cases for domestic travel within the U.S. at the time of this writing, despite 1,600 cases of potentially symptomatic travelers that have been investigated by the CDC.[12] Since contact tracing is difficult when travel is involved due to the decentralized structure of the current efforts, the present study was performed in order to complement the epidemiological data for the purpose of risk assessments.

The amount of respiratory material inhaled by susceptible passengers was quantified in terms of nonvolatile mass and expressed as a percentage of nonvolatile mass expelled by the index subject. This material transport approach is not specific to any disease, and was used because the input data required for a disease transmission model of SARS-CoV-2 and COVID-19 are not currently available. Specifically, the distribution of SARS-CoV-2 across particles of different sizes is not known, but is likely non-uniform: for example, influenza is shed predominantly in smaller particles,[13,14,15] even though larger particles account for the bulk of the expelled volume. Smaller particles also may be more infectious, as they deposit deeper in the respiratory tract upon inhalation. For influenza, the infectious dose may be as much as two orders of magnitude lower for inoculation by inhaled aerosol vs. intranasal drops.[16] These factors are important here because particles of different sizes have different aerodynamic behaviors, so the absence of inputs specific to SARS-CoV-2 and COVID-19 creates a limitation.

Viewed alternatively, the current material transport approach is equivalent to making the simplifying assumptions that the pathogen of interest is distributed uniformly across particles of different sizes, and that the infectious dose is independent of particle size. Given those assumptions, the exposure of susceptible subjects in terms of a percentage of nonvolatile mass expelled would be equivalent to a percentage of viruses expelled, which could then be related to virus shedding rates and infectious doses to extend the present work to a disease transmission model. However, that approach was not selected in the present work because of a low certainty that these simplifying assumptions are valid.

Nonetheless, a key finding of the present work was that the exposure to respiratory particles expelled by the index passenger was low even for the nearest neighbors of the index, with a maximum exposure of 0.3% of the nonvolatile mass expelled. The amount inhaled by the susceptible passengers depended primarily on their proximity to the index and on ventilation, with random fluctuations of the flow field also having a significant role. Relative humidity did not have a substantial effect.

Three ventilation cases were studied that cover the range of ventilation flow rates that would be expected over the course of a journey, with 77% being the average. The lowest flow rate studied, 55% of flow, may occur on the ground during boarding and deplaning segments, when both the engines and the auxiliary power unit (APU) are off, and no ground air supply is available.[A] While this scenario is unlikely, it provided a lower bound for calculating exposures of susceptible passengers to an infected index case. Decreasing the ventilation flow rate increased the dispersion of expiratory particles in the cabin, but did not increase the maximum exposure to the expiratory material. While exposures of passengers seated away from the index increased, exposures of the index's neighbors remained the same within variability due to random flow field fluctuations. For passengers seated away from the index, exposure remained on par or lower than exposure of passengers seated in the same triplet of seats as the index.

The present results are broadly consistent with the results of experimental work[17] that was funded by the United States Transport Command (TRANSCOM) and Air Mobility Command (AMC) divisions of the

[A] Boeing recommends that the APU be operated while on the ground for enhanced safety.

US military, and was planned and carried out by a large team that included some of the authors of the present paper. In that work, tracer aerosols were released at various seat locations throughout Boeing 777-200 and 767-300 airframes, both on the ground and in flight, and were measured at 40+ sensor locations for each release in a manner that represented the breathing of susceptible passengers. A total of over 300 releases were performed. Exposure levels of susceptible passengers were below 0.1% in the vast majority of cases, which was lower than exposure levels in the present model.

The results of this study and those by the TRANSCOM/AMC team were within the same order of magnitude, and the differences are thought to be due to some of the methodological differences, which are summarized in Table 3. The choice of a larger tidal volume in the model explains 50% of the difference. The value in the TRANSCOM/AMC work was selected to represent an average property across the population, while the value here was selected to represent an individual on the higher end of the distribution. In general, tidal volume, and, therefore, the amount of material inhaled depends on gender, age, body mass, and individual factors; however, whether tidal volume affects disease transmission is not yet well understood. The present model used a value on the higher end of the distribution as a conservative assumption. For the same reason, no provision was made to re-exhale a fraction of the inhaled material.

While the choice of tidal volume explains a part of the difference, other factors are required to explain the remainder. One possibility is that, since the experimental releases represented breathing rather than coughing and were thus performed at a slower rate, they presented less of a challenge to the ventilation system than a cough due to their lower inertia, and were removed from the cabin with greater efficiency. Another possibility is that the differences in particle properties or in thermal output of susceptible subjects played a role. A validation study would be required to assess these factors and to identify the reasons for the discrepancy.

Finally, differences due to random fluctuations of the flow field had a larger effect on model results than on TRANSCOM/AMC testing. This can be explained by the differences in release durations: Since the particles were released over a longer time in the experimental work in order to model breathing, over 1 minute compared to 0.4 seconds. This had the effect of averaging over much of the random fluctuation, which was 30 to 120 seconds for the cases studied in the model.

Table 3. Comparison of methods and results in the present work to experimental aerosol releases performed by the TRANSCOM/AMC team[17]

	Property	Present Model	Experimental
Aircraft	Airframe	Boeing 737-800 NG or Boeing 737-8 MAX	Boeing 777-200 and Boeing 767-300
	Airframe type	Narrow-body	Wide-body
	Ventilation flowrate	55%, 77%, 100% flow rate	Similar to 77% flow rate
	PAOs	Off	Off in the majority of cases
Expiratory Particles	Size distribution	Poly-disperse, based on voluntary coughs of healthy volunteers[6]	Narrowly-disperse 1µm nominal (fluorescent)
	Nonvolatile fraction	10%	Polystyrene latex process beads in water
	Interactions with surfaces	100% adhesion on contact	Some adhesion on contact[18]
	Release volume	0.0544 µL	0.0942 µL
	Release duration	0.4 seconds	1 minute
	Tidal volume of susceptible subjects	11.8 L/min	7.5 L/min continuous
	Heat output of susceptible subjects	70W/subject	Negligible for most conditions, 40W/subject for 12 of the test configurations
Results	Exposure (% of release), Average	0.05% for 77% flow rate, 0.05% overall	0.01%
	Exposure (% of release), Maximum	0.24% for 77% flow rate, 0.3% overall	0.22%
	Coefficient of variance, Maximum	45%	15%
	Coefficient of variance, Average	5.4%	9.2%

Conclusion

Seven computational fluid dynamics simulations evaluating the effect of an unmitigated cough were performed on a 5-row model of a 737 cabin. A cough scenario was chosen for the large number of particles generated and because it enabled analysis of the particle mass over time.

The total mass of particles inhaled was dependent on the seat position, air supply rate, and initial steady-state air flow solution. For the conditions run, the highest mass inhaled was 0.3% of that emitted by the cough.

The ultimate fate of particles released in the cabin was the same under all three initial air flow solutions and seat positions. Approximately 50% was deposited on surfaces within the cabin where they no longer provided an inhalation risk. Overall, including both surface deposition and removal by the ECS system, 95% were removed from the air in 2.3-2.5 minutes (80% in 1.3-1.4 min, 99% in 3.3-3.5 min). Reductions in supply air flow rate resulted in a longer time for particle removal from the cabin. Of the cases studied, it took a maximum of 4.5 minutes to reach 95% removal of airborne particle count (80% in 2.6 min, 99% in 6.3 minutes).

Results were consistent with experimental work in which releases of tracer aerosols throughout Boeing 777-200 and 767-300 airplanes were monitored from 40+ seats, with over 300 releases performed using different conditions, including ones on the ground and others in flight.[17] The fraction of material inhaled was lower experimentally than in the model, possibly because of conservative choices that were made in developing the model. The experimental conditions were selected to represent breathing while the model focused on particles released by a cough as a potentially greater challenge to the ventilation system. The model also used a larger tidal breathing volume for susceptible passengers. While other differences between the model and the experimental work existed, a validation study would be required to assess their effects.

As was demonstrated in the previous work by Pang (2020),[19] the risk of contracting COVID-19 while flying is low. Engineering controls on modern aircraft that employ high air flow from ceiling to floor, HEPA filtration, and seat design/positioning that minimize air flow between rows, all play an important role in the control of particle fate in the cabin.

Future work by these authors will examine the relationship between the aircraft cabin and common commercial spaces where engineering controls are less capable of removing particles from the atmosphere.

Acknowledgements:

The authors wish to thank Chao-Hsin Lin for many productive discussions on CFD modeling, and the content and organization of this paper. We wish to acknowledge ANSYS™ for providing licenses for their Fluent™ platform software to support the Confident Travel Initiative studies.

Supplemental Information and Supporting Data

The Cough

Figure 11 illustrates the Cough Peak Flow Rate (CPFR), Peak Velocity Time (PVT), and Cough Expired Volume (CEV) and the particle sizes distribution is shown in Figure 12.

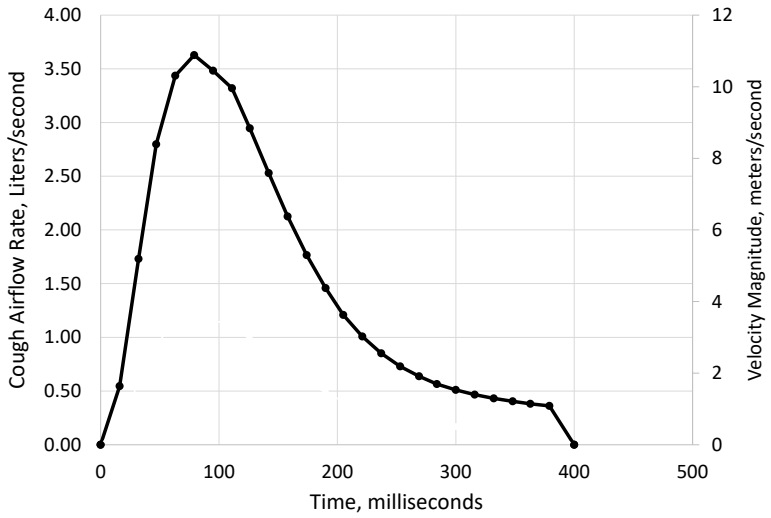

Figure 11. Cough emission characteristics used in simulation. Adapted from Gupta (2009).

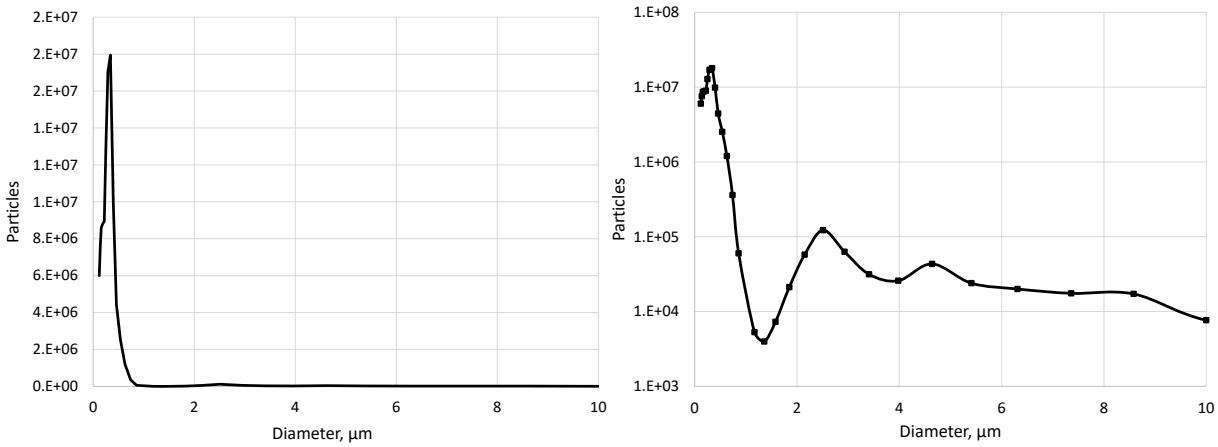

Figure 12. Particle size distribution used in simulation shown on (a) linear and (b) log scale. Adapted from Zayas (2012)[6].

Nonvolatile Mass Inhaled

Seat maps for nonvolatile mass inhaled for each seat location and all seven simulations are displayed in Figure 13 by percent, and in Figure 14 by mass.

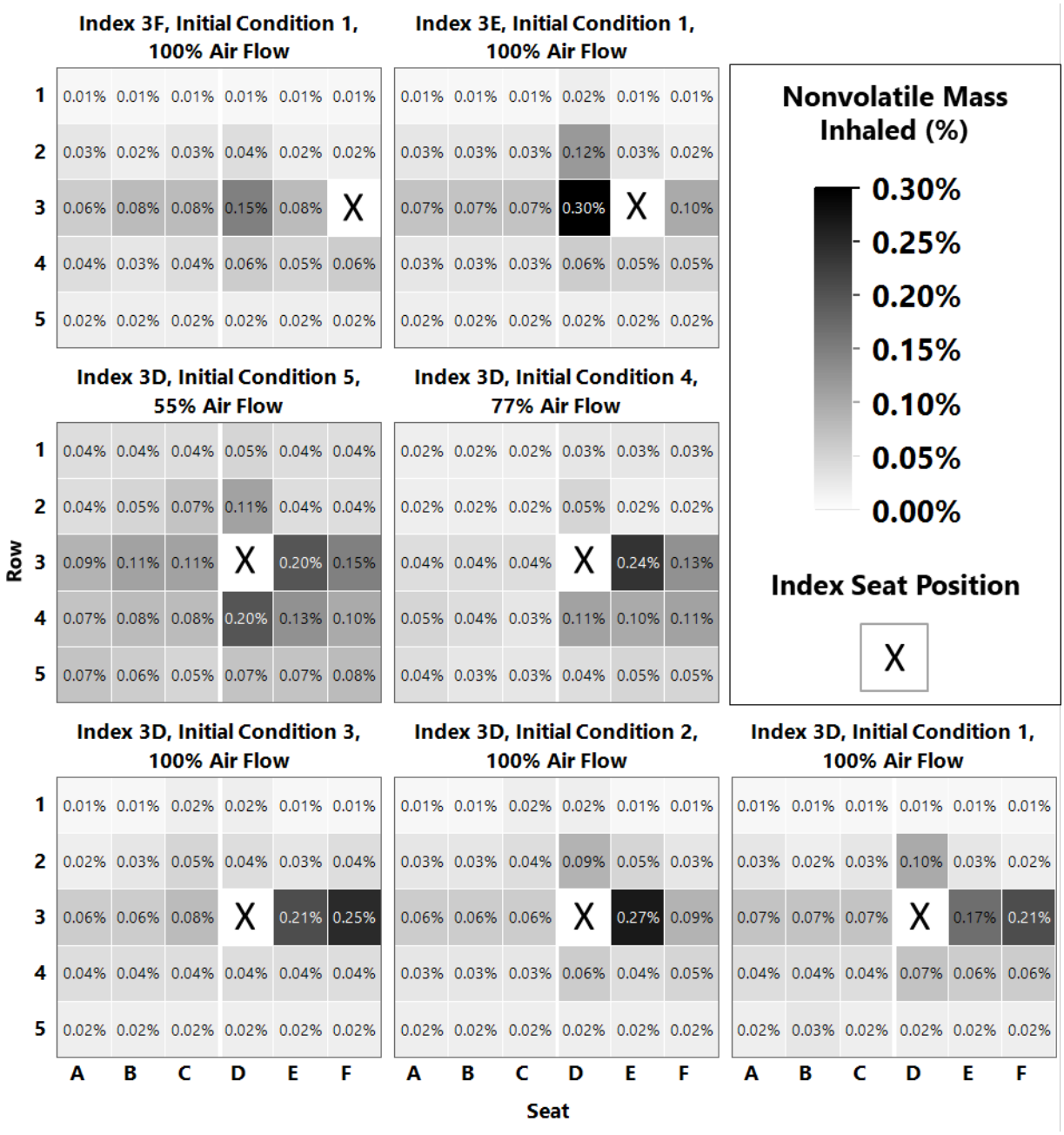

Figure 13 Seat maps of nonvolatile mass inhaled by percent

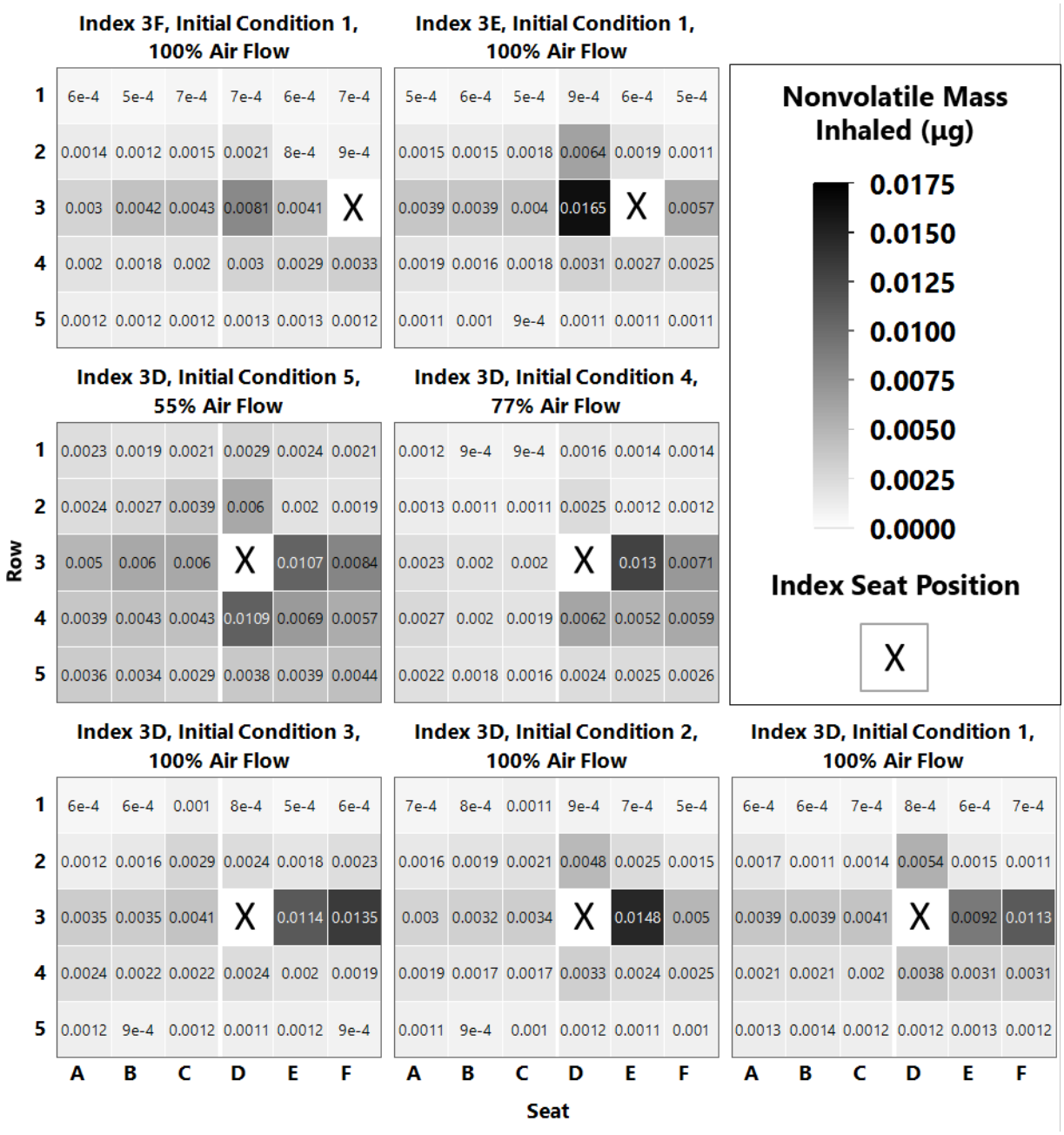

Figure 14 Seat maps of nonvolatile mass inhaled

References and Notes

[1] CDC, Coronavirus Disease 2019 (COVID-19), Symptoms of Coronavirus. https://www.cdc.gov/coronavirus/2019ncov/symptoms-testing/symptoms.html. Accessed 9:31AM 10/29/2020

[2] Code of Federal Regulations, Title 14 - Aeronautics and Space, Subchapter C – AIRCRAFT, Section 25.831 – Ventilation, *Federal Register*, January 1 (2011)

[3] D. J. Tritton, Section 22.7, The Coandă Effect in *Physical Fluid Dynamics*, Van Nostrand Reinhold, (1977)

[4] ASHRAE Standard 52.2-2017 -- Method of Testing General Ventilation Air-Cleaning Devices for Removal Efficiency by Particle Size (ANSI Approved). https://www.techstreet.com/ashrae/standards/ashrae-52-2-2017?product_id=1942059. Accessed 3:15PM PST October 11th 2020

[5] ASHRAE Standard 62.1-2016 -- Ventilation for Acceptable Indoor Air Quality (ANSI Approved). https://www.techstreet.com/ashrae/standards/ashrae-62-1-2016?product_id=1912838. Accessed 3:13PM PST October 11th 2020

[6] G. Zayas, M. C. Chiang, E. Wong, E. Cough aerosol in healthy participants: fundamental knowledge to optimize droplet-spread infectious respiratory disease management. *BMC Pulm Med* **12**, 11 (2012). https://doi.org/10.1186/1471-2466-12-11.

[7] L. Morawskaa, G.R. Johnson, Z.D. Ristovski, M. Hargreaves, K. Mengersen, S. Corbett, C.Y.H. Chao, Y. Lid, D. Katoshevski. Size distribution and sites of origin of droplets expelled from the human respiratory tract during expiratory activities; *Journal of Aerosol Science*; **40**, 3, 256-269 (March 2009).

[8] E. P. Vejerano EP, L. C. Marr. Physico-chemical characteristics of evaporating respiratory fluid droplets. *J. R. Soc. Interface* **15**, 20170939, (2018). http://dx.doi.org/10.1098/rsif.2017.0939

[9] J. K. Gupta, C.-H. Lin, and Q. Chen. Flow dynamics and characterization of a cough, *Indoor Air*, **19**, 517–525 (2009).

[10] J. K. Gupta. Respiratory exhalation/inhalation models and prediction of airborne infection risk in an aircraft cabin, Ph.D. Thesis, Purdue University, West Lafayette, IN (2010)

[11] CDC, National Center for Health Statistics, Body Measurements. https://www.cdc.gov/nchs/fastats/body-measurements.htm. Accessed: 10:07AM PST October 29th 2020.

[12] I. Duncan, Nearly 11,000 people have been exposed to the coronavirus on flights, the CDC says, *The Washington Post*, (Sept. 19, 2020). www.washingtonpost.com/local/trafficandcommuting/nearly-11000-people-have-been-exposed-to-the-coronavirus-on-flights-the-cdc-says/2020/09/19/d609adbc-ed27-11ea-99a1-71343d03bc29_story.html.

[13] W. G. Lindsley, F. M. Blachere, R. E. Thewlis, A. Vishnu, K. A. Davis, G. Cao, J. E. Palmer, K. E. Clark, M. A. Fisher, R. Khakoo, D. H. Beezhold, Measurements of airborne influenza virus in aerosol particles from human coughs. *PLoS ONE* **5**, 11, e15100 (2010).

[14] D. K Milton, M. P. Fabian, B. J. Cowling, M. L. Grantham., J. J. McDevitt, Influenza virus aerosols in human exhaled breath: particle size, culturability, and effect of surgical masks. *PLoS Pathog* **9**, 3, e1003205 (2013).

[15] N. H. L. Leung, D. K. W. Chu, E. Y. C. Shiu, K. –H. Chan, J. J. McDevitt, B. J. P. Hau, H. -L. Yen, Y. Li, D. K. M. Ip, J. S. M. Peiris, W. -H Seto., G. M. Leung, D. K. Milton, B. J. Cowling, Respiratory virus shedding in exhaled breath and efficacy of face masks. *Nat Med* **26**, 5, 676-80 (2020)

[16] R. Tellier, Review of aerosol transmission of influenza A virus. *Emerg Infect Dis* **12**, 11, 1657-62 (2006).

[17] United States Transport Command. TRANSCOM/AMC Commercial Aircraft Cabin Aerosol Dispersion Tests. (2020). https://www.us.transcom.mil/cmd/docs/TRANSCOM%20Report%20Final.pdf. Accessed 4:52PM October 16th 2020.

[18] N. A. Olson, K. J. Skogerboe, R. E. Synovec, Hydrophobic interaction chromatography coupled with dynamic surface tension detection for the determination of surface active species in protein formulations. *J Chromatogr A* **806**, 2, 239-50.

[19] J. Pang, S. P. Jones, L. L. Waite, N. A. Olson, R. Atmur, J. J. Cummins. Probability and Relative Risk of SARS-CoV-2 Transmission on an Aircraft. In preparation. *Unpublished Report,* Boeing internal (2020).